05,08

Magnetic properties of Insb films obtained by laser deposition

© A.I. Dmitriev[1], L.S. Parshina[2], M.S. Dmitrieva[1], O.D. Khramova[2], O.A. Novodvorsky[2]

[1] Federal Research Center of Problems of Chemical Physics and Medicinal Chemistry RAS, Chernogolovka, Russia
[2] Federal State Budgetary Institution „National Research Center „Kurchatov Institute", Moscow, Russia

E-mail: aid@icp.ac.ru

Received December 2, 2024
Revised December 3, 2024
Accepted December 4, 2024

The magnetic properties of InMnSb films obtained by pulsed laser deposition were studied. The temperature dependences of the magnetic moment of the films $M(T)$ cooled in zero magnetic field (ZFC) and a magnetic field of 50 kOe (FC) were measured in different magnetic fields. Analysis of the obtained magnetic data showed that the films consist of two magnetic subsystems: the ferromagnetic subsystem of MnSb nanoinclusions and the paramagnetic subsystem of dispersed Mn^{2+} ions in the InSb matrix. Approximation of the $M(T)$ dependence of the paramagnetic fraction by the Curie–Weiss function made it possible to estimate the concentration of dispersed Mn^{2+} impurity ions $n_i = (6.8 \pm 0.5) \cdot 10^{19}\,\mathrm{cm}^{-3}$, which significantly exceeds the solubility limit of manganese impurity in bulk InSb crystals. As a result of analysis of the $M(T)$ curve of the ferromagnetic phase of MnSb nanoinclusions within the framework of the Bloch 3/2 law, the saturation magnetization $M_S = 225 \pm 24\,\mathrm{emu/cm}^3$ $(1.1 \pm 0.1\,\mu\mathrm{B/ion})$ and the Curie temperature $T_C = 529 \pm 6\,\mathrm{K}$ of MnSb nanoinclusions were determined. The values of both quantities turned out to be significantly lower than in massive single-crystal samples. Analysis of FC–ZFC dependences measured in different fields allowed us to establish the dependence of the blocking temperature T_b of MnSb nanoinclusions on the external magnetic field strength H. Approximation of the $T_b(H)$ dependence allowed us to estimate the field values $H_a = 812 \pm 265\,\mathrm{Oe}$ and the magnetic anisotropy constants $K = (1.1 \pm 0.3) \cdot 10^5\,\mathrm{erg/cm}^3$, which turned out to be close to the corresponding value determined earlier for Mn_xSb_{1-x} single crystals of non-stoichiometric composition $x = 52.8\%$.

Keywords: diluted magnetic semiconductors, InMnSb, pulsed laser deposition.

DOI: 10.61011/PSS.2025.01.60596.332

1. Introduction

The search for high-temperature ferromagnetic diluted magnetic semiconductors is primarily conducted among compounds with the lowest lattice parameters and the widest bandgaps. GaMnAs, GaMnN and InMnN, which have the highest Curie temperatures are such compounds among the semiconductors of III-Mn-V family. Despite the large number of publications devoted primarily to GaMnAs, many questions remain open, and even the basic mechanism of ferromagnetism in III-Mn-V is often only qualitatively understood. Under these conditions, we believe that much can be learned by studying the opposite edge of III-Mn-V family, referring to the InMnSb compound, which has the largest lattice constant and the smallest band gap. From a practical point of view, the narrow band gap of InMnSb opens up prospects for infrared spin photonics. It is also possible to expect an improvement in the transport of charge carriers owing to the lower effective mass of holes and their higher mobility [1]. Even if it turns out to be non-ferromagnetic, the InMnSb compound can be successfully used as a material for ultra-low temperature thermistors [2] and magnetic field sensors [3].

The early compound InMnSb was studied being prepared in various ways. The first InMnSb samples were produced as films by low-temperature molecular beam epitaxy [1,4]. Their Curie temperatures did not exceed 8 K [1] and 20 K [4]. The samples obtained using the controlled annealing technique had a Curie temperature above 130 K [5]. The Curie temperature exceeded room temperature in films grown by liquid-phase epitaxy [6], as well as in massive InMnSb samples [7–9]. The Curie temperature exceeded 400 K in films grown by the method of organometallic vapor phase epitaxy [10]. Such high Curie temperatures may correspond to nanoinclusions of the secondary phase of MnSb [9], or they may correspond to a subsystem of dispersed exchange-coupled manganese ions combined into dimers, trimers, etc. [11]. The magnetic properties of InMnSb films obtained by pulsed laser deposition (PLD) with high-temperature ferromagnetism are studied in this paper. The PLD method using mechanical droplet separation makes it possible, when sputtering multicomponent substances, to obtain thin films of the composition of the initial target [12], and to ensure nonequilibrium solubility of the components in films of complex composition owing to the high energy of the deposited particles. The purpose of this paper is to study the mechanisms leading to a high-temperature ferromagnetic state, as well as to separate the contributions of various magnetic subsystems to the total magnetization.

2. Experimental techniques and sample preparation

InSb:Mn thin films were synthesized by the PLD method from InSb-MnSb targets of eutectic composition (6.5%) and 15% ratio of manganese to indium. Compositions of InSb-MnSb system were obtained by the Bridgman method using a charge of the appropriate composition. The obtained samples of constant composition consisted of a monocrystalline InSb matrix and monocrystalline MnSb needles with a diameter from 20 to 4 μm, oriented along the growth direction [13]. The target washers were cut from these samples, perpendicular to the direction of growth. InSb:Mn films were synthesized in the PLD mode with mechanical separation of torch particles by radiation from an excimer KrF laser (248 nm) on c-sapphire substrates in vacuum. The use of a drip-free film deposition mode ensures the production of smooth, homogeneous films of high quality at room temperature of the substrate by eliminating droplets flying from the target onto the substrate during film deposition. During film growth, a mechanical separator transmits rapidly flying atoms and ions onto the substrate, but eliminates the ingress of large droplets onto the growing film, the presence of which is the main factor in reducing the quality of the films produced during pulsed laser deposition. The deposition of films with mechanical particle separation is described in more detail in Ref. [14]. The temperature of the substrate ranged from 250°C to 350°C during sputtering.

The dependences of the magnetic moment of the InMnSb films on temperature and magnetic field strength were measured using a CFMS vibration magnetometer (Cryogenic Ltd, UK). The temperature dependences of the magnetic moment were measured for films cooled in a zero magnetic field (ZFC — zero-field cooled) and a magnetic field with a strength of 50 kOe (FC — field cooled).

3. Results and their discussion

Figure 1 shows the temperature dependence of the magnetization $M(T)$ of the InMnSb film, measured in the cooling mode in a magnetic field with a strength of 50 kOe.

Two sections can be distinguished on the curve $M(T)$. The high temperature range of $T > 50$ K, where the magnetization increases smoothly with decreasing temperature. The low temperature region of $T < 50$ K, where the magnetization begins to increase sharply with a further decrease in temperature. A similar magnetization behavior was previously observed for magnetic semiconductors consisting of two phases with different dependencies $M(T)$ for each of the phases [15]. The presence of a ferromagnetic subsystem of MnSb nanoclusions and a subsystem of dispersed ions of Mn^{2+} in the InSb matrix in the sample is typical for systems similar to the studied InMnSb films. The curve $M(T)$ of InMnSb film was analyzed using the sum of two functions — Bloch's law 3/2, which describes the ferromagnetic phase of MnSb nanoclusions, and Curie's law, which describes the paramagnetic phase of dispersed ions Mn^{2+} in the InSb matrix:

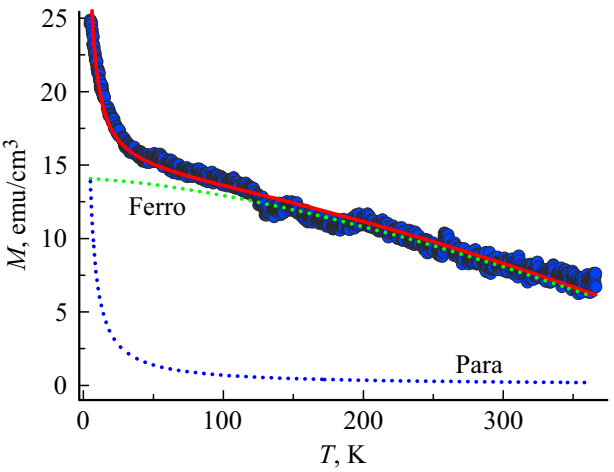

Figure 1. The temperature dependence of the magnetization of the InMnSb film, measured in the cooling mode in a magnetic field with a strength of 50 kOe. The solid line shows the approximation by the expression (1). The dotted lines show the contributions of the paramagnetic (para) and ferromagnetic (ferro) subsystems to the total magnetization.

$$M(T) = \eta M_s \left(1 - \left(\frac{T}{T_C}\right)^{3/2}\right) + (1-\eta)\frac{CH}{T}, \qquad (1)$$

where η is the volume fraction of the ferromagnetic fraction of MnSb nanoclusions in the InMnSb film, T is the temperature, $H = 50$ kOe is the magnetic field strength, M_S is the saturation magnetization of MnSb nanoclusions at $T \to 0$ K, T_C is the Curie temperature of MnSb nanoclusions, C is the Curie constant of the paramagnetic fraction of dispersed ions Mn^{2+} in the InSb matrix. The approximation of the dependence $M(T)$ of InMnSb film by the expression (1) is shown by a solid in Figure 1. The following parameters were determined from the approximation method: $\eta = 0.06 \pm 0.01$, M_S=225 $\pm$ 24 emu/cm^3(1.1 $\pm$ 0.1 μB/ion), T_C=529 $\pm$ 6 K, $C = (1.5 \pm 0.1) \cdot 10^{-3}$ emu $\cdot$ K/Oe $\cdot$ cm^3. The coefficient of determination is $R^2 = 0.98$. The volume fraction of the ferromagnetic fraction of MnSb nanoclusions in the InMnSb film is close to, but slightly higher than, the corresponding value of 0.04 previously found for polycrystalline massive samples of similar composition [11]. The saturation magnetization of MnSb nanoclusions turned out to be more than three times lower than the known value of 770 emu/cm^3 (3.5 μB/ion) for massive single crystal samples [16]. A similar situation was observed earlier in $Mn_{1+x}Sb$ single crystals of nonstoichiometric composition $x = 0.22$ (manganese content 55.3 at.%), in which the saturation magnetization is about one and a half times lower than the corresponding value for stoichiometric crystals of MnSb [16]. The mechanism of this dependence of

the saturation magnetization of MnSb crystals on the composition is as follows. Mn atoms can occupy two positions in the crystal lattice of nonstoichiometric crystals of $Mn_{1+x}Sb$: in lattice sites with a magnetic moment $3.50\,\mu B$ and in the interstices with a magnetic moment $2.38\,\mu B$. Moreover, the spins of the Mn atoms in both positions are directed antiparallel to each other, which leads to a decrease of the saturation magnetization [16]. There is an empirical dependence $M_S = (3.5-5.5x)\,\mu B$, which can be used to estimate the saturation magnetic moment for nonstoichiometric crystals $Mn_{1+x}Sb$ [16,17]. According to this dependence, the saturation magnetization value obtained in this work corresponds to the value $x = 0.43$ (the proportion of manganese is 60.1 at.%). A reduced saturation magnetization to the values of $250-400\,emu/cm^3$ was also previously observed in MnSb nanoparticles with a diameter of $15-30\,nm$ [18] and MnSb films consisting of micron crystallites [19]. The decrease of saturation magnetization in these situations is caused by breaking of exchange bonds on the surface of nanoparticles or at the grain boundary. The value of the Curie temperature of MnSb nanoclusions also turned out to be lower than the known value of 587 K for massive single crystal samples [16,20]. This may also be caused by the non-stoichiometry of the nanoclusions. The Curie temperature decreases almost linearly with the increase of x according to the data of [16] for nonstoichiometric crystals of $Mn_{1+x}Sb$. The value of the Curie constant C of the paramagnetic fraction according to the formula $n_i = 3Ck_B/\mu_B^2 g^2 S(S+1)$ allows estimating the concentration of dispersed impurity ions of Mn^{2+} $n_i = (6.8 \pm 0.5) \cdot 10^{19}\,cm^{-3}$. Here k_B is the Boltzmann constant, μ_B is theBohr magneton, $g = 2$ is g-factor, $S = 5/2$ is the spin. The concentration of dispersed impurity ions Mn^{2+} n_i is close to the corresponding value of $(2-9) \cdot 10^{19}\,cm^{-3}$, previously found for polycrystalline massive samples of similar composition [11]. It significantly exceeds the solubility limit of Mn manganese impurity in massive crystals of indium antimonide InSb, which does not exceed $(0.5-1) \cdot 10^{19}\,cm^{-3}$ [11]. A similar situation was observed earlier in epitaxial films of $In_{1-x}Mn_xSb$ [10]. Typically, an increase of the solubility limit occurs during sample preparation under highly nonequilibrium conditions.

The temperature dependences of the magnetization of InMnSb films cooled in a zero magnetic field and a magnetic field (ZFC) with a strength of 50 kOe (FC) were measured to determine the blocking temperature T_b (Figure 2). Figure 2 shows the following behavior of curves $M_{ZFC}(T)$ and $M_{FC}(T)$, which is typical for superparamagnetic nanoclusions of MnSb. They coincide at sufficiently high temperatures, but begin to differ below a certain temperature of irreversibility. In this case, the curve $M_{ZFC}(T)$ has a maximum at a certain temperature, and $M_{FC}(T)$ increases monotonously up to the lowest temperatures. It is easy to qualitatively understand the reason for the different behavior in our ZFC and FC experiments for an idealized MnSb superparamagnetic nanoinclusions system containing identical nanoparticles with uniaxial anisotropy

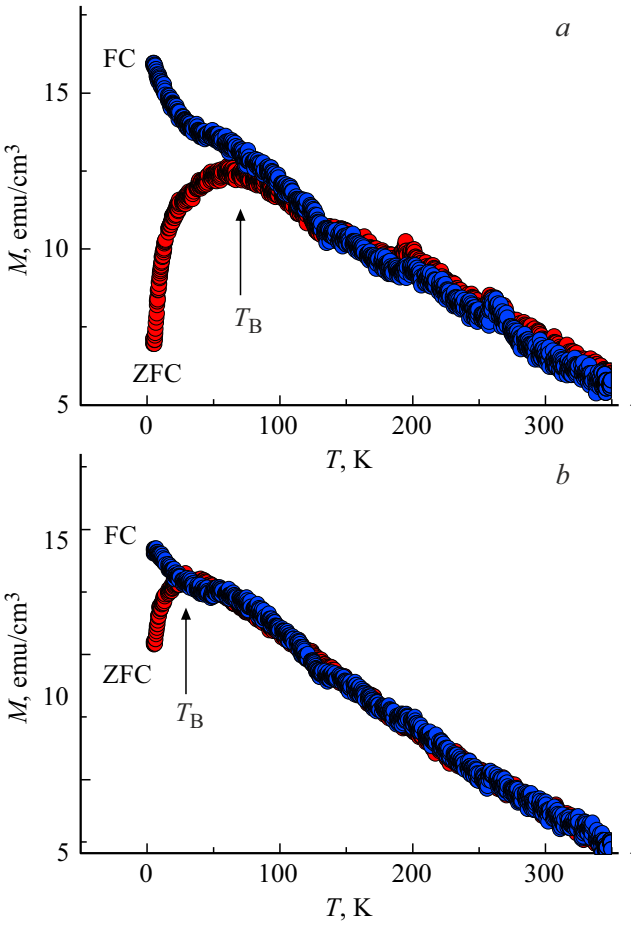

Figure 2. Temperature dependences of the magnetic moment of InMnSb films cooled in a zero magnetic field — ZFC (red symbols) and a magnetic field with a strength of 50 Ke — FC (blue symbols). The measurements were conducted in magnetic fields with a strength of 400 Oe (a) and 800 Oe (b).

and random orientation of the easy axes [21]. In the first case, when cooled below the blocking temperature T_b, the magnetic moments of MnSb nanoinclusions are directed along their easy axes (angle θ between the direction of the particle's magnetization vector and the axis of anisotropy is zero). The total magnetic moment of the system is zero, both at the beginning of the cooling process and at the end of it.

When the measuring magnetic field is turned on, the magnetic moments for which $\theta < 90^\circ$ do not need to overcome the energy barrier for transition to a position with minimal energy. These magnetic moments create a nonzero magnetization of the system by slightly turning. On the contrary, particles for which the condition $\theta > 90^\circ$ is fulfilled at the moment of switching on the magnetic field are separated from the minimum potential energy by a barrier, which they can overcome only in a very long time. Therefore, the system has a metastable state with a small total magnetic moment at $T < T_b$ in case of ZFC measurements. If the temperature is increased, then the

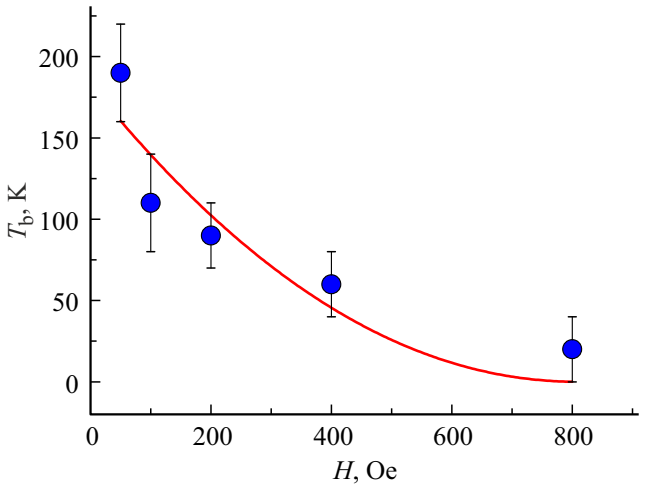

Figure 3. Dependence of the blocking temperature T_b on the magnetic field strength H. The solid line shows the approximation.

system will jump into a stable superparamagnetic state at $T = T_b$. In case of FC measurements, the sample is cooled in a nonzero magnetic field and the magnetization at all temperatures above T_b behaves like during ZFC measurements. But the system can no longer change its magnetization during measurements at $T < T_b$, therefore $M_{FC} = \text{const}$ below the blocking temperature. In our case, the MFC value continues to grow due to the contribution of the hyperbolic temperature dependence of the paramagnetic fraction of dispersed ions of Mn^{2+}. For a system consisting of single-domain nanoparticles with different size, shape, etc., the curves $M_{ZFC}(T)$ and $M_{FC}(T)$ are separated not at $T = T_b$, but at a higher temperature, which is called the point of irreversibility. Another characteristic point is the maximum on the curve $M_{ZFC}(T)$, which is often identified with the average system blocking temperature. The temperature of irreversibility can be associated with T_b for particles of maximum size.

Figure 3 shows the dependence of the blocking temperature T_b on the magnetic field strength H. The blocking temperature T_b decreases from 190 K to 20 K with an increase of the magnetic field strength H from 50 Oe to 800 Oe.

The physical mechanism of this is as follows. In the absence of an external magnetic field, the energy barrier caused by magnetic anisotropy and separating the directions of the magnetic moment „up“ and „down“is equal to $E = KV$. The energy barrier E_{ap} preventing the magnetic moment from turning from an antiparallel direction relative to the magnetic field strength in parallel direction, decreases from $E = KV$ to $E_{ap}(H) = KV - mH$ in case of application of the external magnetic field with a strength H which is small compared to the magnetic anisotropy field H_a and directed along the axis of light magnetization. On the contrary, the energy barrier E_{pa} preventing the magnetic moment from turning from a parallel direction relative to the magnetic field strength to an antiparallel direction, increases from $E = KV$ to $E_{pa}(H) = KV + mH$. Since $E_{ap} > E_{pa}$, magnetic moment rotations caused by thermal fluctuations from an antiparallel direction to a parallel direction become more likely than the reverse ones. This leads to an increase of the initial value of the magnetization on the curve M_{ZFC}. As a result, the measured value of the blocking temperature T_b, attributable to the magnetic moment rotations discussed above caused by thermal fluctuations, decreases. A rigorous analysis of the impact of an external magnetic field on the value of the energy barrier leads to the expression $E(H) = KV[1(H/H_a)]^2$, here $H < H_a$, and the signs „–“ and „+“ correspond to the rotation of the magnetic moment from an antiparallel direction to a parallel one and vice versa, respectively. Substituting the expression $E(H)$ into the known formula for the blocking temperature leads to the expression for the dependence $T_b(H)$ [22,23]:

$$T_b = T_{b0}\left(1 - \frac{H}{H_a}\right)^2, \qquad (2)$$

Here T_{b0} is the blocking temperatures in the absence of a magnetic field, H is the external magnetic field strength, H_a is the magnetic anisotropy field.

A solid line in Figure 3 shows the approximation of the dependence $T_b(H)$ by the expression (2). The values $T_{b0} = 183 \pm 30$ K and $H_a = 812 \pm 265$ Oe were determined from the approximation. The relatively low quality of the fit (coefficient of determination $R_2 = 0.84$) and the relatively large relative error of determining the values of T_{b0} (16%) and H_a (33%) may be attributable to the spread of the easy axes in space, the distribution of by size or by dipole-dipole interaction.

Knowing the values of H_a and M_s from the known ratio $H_a = 2K/M_s$, we can estimate the value of the magnetic anisotropy constant $K = (1.1 \pm 0.3) \cdot 10^5$ erg/cm^3. The obtained value of K is close to the corresponding value previously determined for single crystals Mn_xSb_{1-x} of nonstoichiometric composition $x = 52.8\%$ [16].

Knowing the values of T_{b0} and K from the known ratio $T_{b0} = KV/25\,\text{kB}$, we can estimate the average values of the volume V and the diameter of the MnSb nanoclusions $D = 28 \pm 4$ nm.

4. Conclusion

The contributions to the total magnetization of InMnSb films from the ferromagnetic subsystem of MnSb nanoinclusions and the paramagnetic subsystem of dispersed ions Mn^{2+} in the InSb matrix are separated. The saturation magnetization and Curie temperature of MnSb nanoinclusions were determined, which turned out to be noticeably lower than in massive single-crystal samples. This can be caused either by the breaking of exchange bonds on the surface of nanoclusions or at the grain boundary, or by their nonstoichiometry. The concentration of Mn^{2+} ions in the paramagnetic subsystem significantly exceeds

the solubility limit of the manganese impurity in massive InSb crystals. This is probably attributable to the highly nonequilibrium conditions in which samples are produced by pulsed laser deposition. The magnitude of the coercive force of MnSb nanoclusions is close to the corresponding value for both MnSb films and MnSb nanoparticles obtained earlier by various methods, and is noticeably lower than the magnetic anisotropy field of MnSb nanoclusions. The value of the magnetic anisotropy constant was estimated, which turned out to be close to the corresponding value previously determined for single crystals Mn_xSb_{1-x} of nonstoichiometric composition $x = 52.8\%$. The average value of the diameter of the MnSb nanoclusions was estimated from the magnetometric data.

Acknowledgments

The authors would like to express their gratitude to A.V. Kochura and B.A. to Aronzon for stimulating discussions.

Funding

Regarding the synthesis of thin films, the study was conducted under the state assignment of National Research Center „Kurchatov Institute“. With regards to the study of magnetic properties the study was conducted under the state assignment of the Federal Research Center for Problems of Chemical Physics and Medical Chemistry of the Russian Academy of Sciences (124013100858-3).

Conflict of interest

The authors declare that they have no conflict of interest.

References

[1] T. Wojtowicza, W.L. Lim, X. Liu, G. Cywinski, M. Kutrowski, L.V. Titova, K. Yee, M. Dobrowolska, J.K. Furdyna, K.M. Yu, W. Walukiewicz, G.B. Kim, M. Cheon, X. Chen, S.M. Wang, H. Luo, I. Vurgaftman, J.R. Meyer. Physica E **20**, *3–4*, 325 (2004).
[2] S.A. Obukhov, B.S. Neganov, Y. Kiselev, A.N. Chernikov, V.S. Vekshina, N.I. Pepik, A.N. Popkov. Cryogenics **31**, *10*, 874 (1991).
[3] D.L. Partin, J. Heremans, C.M. Thrush. J. Crystal Growth **175-176**, *2*, 860 (1997).
[4] S. Yanagi, K. Kuga, T. Slupinski, H. Munekata. Physica E **20**, *3–4*, 333 (2004).
[5] J. Hollingswort, P.R. Bandaru. Mater. Sci. Eng. B **151**, *2*, 152 (2008).
[6] K. Ganesan, S. Mariyappan, H.L. Bhat. Solid State Commun. **143**, *4–5*, 272 (2007).
[7] K. Ganesan, H.L. Bhat. J. Appl. Phys. **103**, *4*, 043701 (2008).
[8] V.A. Ivanov, O.N. Pashkova, E.A. Ugolkova, V.P. Sanygin, R.M. Galera. Neorgan. materialy **44**, *10*, 1168 (2008). (in Russian).
[9] E.I. Yakovleva, L.N. Oveshnikov, A.V. Kochura, K.G. Lisunov, E. Lakhderanta, B.A. Aronzon. Pis'ma v ZhETF **101**, *2*, 136 (2015). (in Russian).
[10] N.D. Parashar, N. Rangaraju, V.K. Lazarov, S. Xie, B.W. Wessels. Phys. Rev. B **81**, *11*, 115321 (2010).
[11] A.V. Kochura, B.A. Aronzon, K.G. Lisunov, A.V. Lashkul, A.A. Sidorenko, R. De Renzi, S.F. Marenkin, M. Alam, A.P. Kuzmenko, E. Lahderanta. J. Appl. Phys. **113**, *8*, 083905 (2013).
[12] S.F. Marenkin, O.A. Novodvorsky, A.V. Shorokhova, A.B. Davydov, B.A. Aronzon, A.V. Kochura, I.V. Fedorchenko, O.D. Khramova, A.V. Timofeev. Neorgan. materialy **50**, *9*, 973 (2014). (in Russian).
[13] S.F. Marenkin, A.V. Kochura, I.V. Fedorchenko, A.D. Izotov, M.G. Vasiliev, V.M. Trukhan, E.V. Shelkova, O.A. Novodvorsky, A.L. Zheludkevich. Neorgan. materialy **52**, *3*, 309 (2016). (in Russian).
[14] L.S. Parshina, O.A. Novodvorsky, O.D. Khramova, I.A. Petukhov, A.A. Lotin, V.S. Mikhalevsky, A.V. Shorokhova. Comp. nanotechnol. **1**, 62 (2014).
[15] A.I. Dmitriev, R.B. Morgunov, O.L. Kazakova, Y. Tanimoto. ZhETF **135**, *6*, 1134 (2009). (in Russian).
[16] T. Okita and Y. Makino. J. Phys. Soc. Jpn., **25**, *1*, 120 (1968).
[17] R. Coehoorn, C. Haas, R.A. de Groot. Phys. Rev. B **31**, *4*, 1980 (1985).
[18] H. Zhang, S.S. Kushvaha, S. Chen, X. Gao, D. Qi, A.T.S. Wee, X.-S. Wang. Appl. Phys. Lett. **90**, *20*, 202503 (2007).
[19] B.L. Low, C.K. Ong, J. Lin, A.C.H. Huan, H. Gong, T.Y.F. Liew. J. Appl. Phys. **85**, *10*, 7340 (1999).
[20] K. Lawniczak-Jablonska, A. Wolska, J. Bak-Misiuk, E. Dynowska, P. Romanowski, J.Z. Domagala, R. Minikayev, D. Wasik, M.T. Klepka, J. Sadowski, A. Barcz, P. Dluzewski, S. Kret, A. Twardowski, M. Kamińska, A. Persson, D. Arvanitis, E. Holub-Krappe, A. Kwiatkowski. J. Appl. Phys. **106**, *8*, 083524 (2009).
[21] S.P. Gubin, Yu.A. Koksharov, G.B. Khomutov, G.Yu. Yurkov. Uspekhi khimii **74**, *6*, 539 (2005). (in Russian).
[22] Y.D. Zhang, J.I. Budnick, W.A. Hines, C.L. Chien, J.Q. Xiao. Appl. Phys. Lett. **72**, *16*, 2053 (1998).
[23] M. Knobel, W.C. Nunes, H. Winnischofer, T.C.R. Rocha, L.M. Socolovsky, C.L. Mayorga, D.Zanchet. J. Non-Cryst. Solids **353**, *8–10*, 743 (2007).

Translated by A.Akhtyamov